

Investigation of Effects of Heater Tube Angle on the Pool Boiling Heat Transfer Coefficient

Khooshehchin, Mohsen

Department of Chemical Engineering, Kermanshah Branch, Islamic Azad University, Kermanshah, I.R. IRAN

Fathi, Sohrab*⁺

Department of Chemical Engineering, Faculty of Engineering, Kermanshah University of Technology, Kermanshah, I.R. IRAN

Salimi, Farhad*

Department of Chemical Engineering, Kermanshah Branch, Islamic Azad University, Kermanshah, I.R. IRAN

Ovaysi, Saeed

Faculty of Petroleum and Chemical Engineering, Razi University, Kermanshah, I.R. IRAN

ABSTRACT: *In this experimental study, the effects of slope changes on the heat transfer coefficient in pool boiling in deionized water have been investigated. The experiments were carried out in the average surface roughness of 0.21 μm on a copper cylinder by changing the surface slope including 0°, 5°, 10°, 15°, 20°, 25°, and 30°. The range of heat flux was from 21 to 77 kW/m in atmospheric conditions. The results indicated that by increasing the heater slope, the departure frequency and bubble departure diameter on the heater surface were increased which lead to an increase in the mixing, turbulence, and heat transfer coefficient. Finally, the slope of 15° has reached the highest heat transfer coefficient with an increase of 20.09% compared to other slopes. Besides the optimized model was mostly overlapped with the experimental results in which Stephan Abdelsalam's model with an average error of 13.9% and the McNelly model with an average error of 24% had the minimum and maximum amount of error among the other models, respectively.*

KEYWORDS: *Pool boiling; Heat transfer coefficient; Bubble departure frequency; Bubble departure diameter; Slope of the surface.*

INTRODUCTION

Boiling heat transfer is an efficient heat transfer method that is extensively utilized in various fields such as electricity generation, electronic devices, cooling systems, producing chemical substances, management of

active heating systems, power cycle, and storage and transfer of the cryogenic liquids in the chamber. Design, operation, and optimization of the involved equipment necessitate an accurate prediction of the boiling heat

* To whom correspondence should be addressed.

+ E-mail: s.fathi@kut.ac.ir ; f.salimi@iauksh.ac.ir
1021-9986/2022/3/957-970 14/\$/6.04

transfer between the surface and the boiling liquid [1]. An important advantage of the boiling heat transfer system is that a great of heat could be transferred from a level with a higher temperature to a liquid with a lower temperature, even with a little superheat (temperature difference between the heat transfer surface and the solution in contact with it), in comparison with the natural or forced heat transfer methods which are without phase-changing. However, heat dissipation capacity is limited by an upper cooling limit named Critical Heat Flux (CHF) [2]. In a process, an efficient evaporator can reduce energy consumption, economic resources, and dangers to the environment [3]. The boiling functionality is based on two main parameters which include Boiling Heat Transfer Coefficient (BHTC) and CHF. BHTC is the amount of removed heat from the hot surface, while the CHF is the upper range of nucleate boiling and beyond that, a boiling surface is covered by a vapor film and catastrophic corrosion could be occurred [4]. Current techniques for improving heat transfer can be divided into two categories: Active methods, which need external forces. Passive methods, do not need certain external forces [5].

The structure of the heat transfer surface may be rigorously complicated [6]. Determining the slope of the heat transfer surface is considered to be one of the principal and essential factors in the heat flux, which means that the surface could be vertical, horizontal, and at any particular angle so that the configuration and separation of the generated bubbles could enhance their performance. For this reason, numerous studies by the researchers have been carried out so that each researcher has recommended a specific method to determine the heater surface. The reports have shown that after discharge and raising the surface, the bubble would like to move along the surface for certain distances. However, slider distances, and the movement of the bubble, have not been reported. Therefore, an average slider distance for pool boiling on vertical surfaces is equal to half of the distance between the two closest bubbling sites in one specific area. Depending upon the application, the axis orientation of the boiling tube may be horizontal or vertical [7] and it has been tested experimentally by varying the tube orientation between vertical and horizontal [8-14]. Kang concluded that the tube orientation had a high impact on the HTC, stating that the maximum and minimum of HTC were expected at the horizontal and vertical orientations,

respectively. The cause for the variation was due to changes in bubble slug formation on the tube surface as well as liquid accessibility to the surface [10].

Parker and El-Genk have investigated the effect of surface inclination angle, from 0° to 180° on CHF [16]. Compared to smooth plain copper, the rate of heat transfers by natural convection and CHF increased 68% and as much as 157%, respectively. Kang examined and showed the inclination angle gives much change in heat transfer coefficients and when a tube is near the horizontal and the vertical, the maximum and the minimum heat transfer coefficients are expected, respectively [12]. Zhong et al. [17] and Dadjoo et al. [18] showed that the heat fluxes improve with the wall superheat at each inclination angle and the CHF enhances by the increasing inclination angle. Kang et al. experimentally studied the effects of the slip change of the pool boiling heat transfer on the cylinder surface [13]. They concluded that the heat transfer coefficient is extremely affected by angle changes. When the cylinder is close to the vertical and horizontal modes, the maximum and minimum heat transfer coefficient would be expected. In addition, they believed that the reason for transferring the increased heat is the reduction of mass formation or bubble flocculation in the cylinder surface and the easy accessibility of the liquid to the surface. Priarone conducted some experiments to study the effect of the surface charge on the nucleate boiling in dielectric liquids (HFE-7100 and FC-72) into cylinder surface made of copper [19]. The angle of the copper cylinder in the nucleate boiling zone for both liquids has lower heat flux and the heat transfer coefficient is significantly increased as the angle surges from 0° to 90° . He presented this hypothesis so that the mandatory removal of heat layers of the surface adjacent is caused an increase in bubbles movements throughout the heat transfer surface while the slope is being raised. Jung et al. conducted boiling experiments on one heater with a flat surface into the bath of saturated water under atmospheric pressure [20]. The achieved heat flux depicted that the change of the boiling surface from a horizontal mode to the vertical could lead to an increase in the active nucleation site density. Goel et al. reported that a rise in the heat transfer surface from horizontal to vertical (0° - 90°) could cause to increase in the departing diameter and bubble departure frequency [21]. The main reason could be related to the slide movement of the bubble growing on the inclined

surface before it wants to be raised from the heater surface. This sliding movement can cause to increase in the rate of bubble growth and hence, it can enlarge the bubble of the heater surface and then, it leaves the surface by higher frequencies and as a result, it follows the higher rate of the heat transfer due to the increasing rate of turbulence.

The purpose of this study is to obtain the pool boiling heat transfer coefficient using variations in the angle of placement of the heat transfer surface. To obtain a higher heat transfer coefficient, it is necessary to investigate the treatment of the dynamic parameters of the bubbles. The optimal amount of parameters should be obtained to improve the heat transfer coefficient at an appropriate slope.

Modeling literature survey

In the following, the most important models presented in the field of heat transfer coefficient of pool boiling are presented.

In 1952 *Rohsenow* suggested his model in which the basic assumption was explained on the basis that, the movement of bubbles from the beginning of separation from the heat transfer surface, has the most importance [22]. Also, it is important that claimed the separation of bubbles from the heat transfer surface in solution has caused turbulence and high mixing which causes the improvement in the heat transfer flow and also decreases the thickness of the liquid film layer on the heat transfer surface. *McNally* empirical relationship was introduced in 1953, was presented to calculate the boiling heat transfer coefficient of pure liquids [23]. This model was only acceptable for anticipating pure and single-component liquids. Also, it utilized the physical properties of the liquid phase (boiling) and steam phase. *Kutateladze* an empirical relationship was presented in 1959 [24]. This experimental model computes the heat transfer coefficient due to the application of two dimensionless parameters without considering the average surface roughness profile. *Labanastov* presented the model using various liquids and by repeating the tests in 1963 [25]. Considering that this model was based on a great deal of laboratory data, while more than 200 substances were used to model this relationship, it had a good overlapping with the laboratory. *Stephan* and *Abdelsalam* introduced their well-known equation which was about anticipating the boiling heat transfer coefficient of pure liquids in 1980 [26]. This

equation has been achieved due to the utilization of multiple regression and the great volume of laboratory databases (for over 500 substances). He severely reduced the heat transfer coefficient deviation of experimental data by presenting this relationship. *Nishikawa* [27] presented his experimental model due to the utilization of modifying previous laboratory data. The importance of this model is due to the independence of thermos-physical properties and only by having the test conditions the presentation and analysis of results could be applicable. Cooper introduced his model in 1984 that contained reduced pressure, average surface roughness, and also a molecular mass of fluid, by utilization of 6000 published lab results from various resources which were the deduction of 100 series of the pool boiling transfer coefficient experiment [28]. *Gorefnlo* [29] was the designer and provider of a novel laboratory system for estimating the heat transfer coefficient. In this model, he introduced the boiling heat transfer coefficient subordinated to thermal flux, decreased pressure, and average surface roughness. There is one heat transfer coefficient of pressure and thermal flux included in the main equation that the value of it is calculable experimentally or due to other relationships. *Alavi Faze* declared his model in 2010 according to the principle of the corresponding states and dimensional analysis [30]. It has a good overlap with experimental data in order to calculate the boiling heat transfer coefficient of pure liquids. In 2017 *Kiyomura et al.* expressed that the increase in HTC is related to an increase in liquid turbulence represented their proposed model considering the impression of several test fluids, gap size, and contact angle of a liquid [31]. This developed model is presented based on the Buckingham theorem (π^2) to intensify the selected independent variables to show dependent parameters.

One of the key parameters that are affecting heat transfer rate is bubble departure frequency from the surface which has a close relationship with bubble departure diameter and the mechanisms that govern the bubble growth. This key parameter is defined as the below equation.

$$f = \frac{1}{n} \sqrt{\frac{1}{t_w + t_g}} \quad (1)$$

In which t_g is the time needed for bubble growth from nucleation to separation from surface and t_w is required

Table 1: The proposed relations of the researchers for the heat transfer coefficient.

Model Name	Model
Rohsenow 1951 [22]	$\frac{h\beta'}{K} \left[\frac{g_c \sigma}{g(\rho_l - \rho_v)} \right]^{1/2} = C_r \left[\frac{\beta'}{\mu} \left(\frac{g_c \sigma}{g(\rho_l - \rho_v)} \right)^{1/2} \frac{w}{A} \right]^2 \left(\frac{c\mu}{k} \right)^{-0.7}$
McNelly 1953 [23]	$h = 0.225 \left(\frac{4c\mu}{A H_{fg}} \right)^{0.69} \left(\frac{\rho_l k_l}{\sigma} \right)^{0.31} \left(\frac{\rho_l}{\rho_v} - 1 \right)^{0.33}$
Kutateladze 1959 [24]	$h = [3.37 E \frac{Kl}{I_*} \left(\frac{H_{fg}}{C_{pl} \left(\frac{q}{A} \right)} \right)^{-2} M_*^{-4}]^{1/3}$ $I_* = \left[\frac{\sigma}{g(\rho_l - \rho_v)} \right]^{0.5}$ $\frac{\left(\frac{p}{\rho_v} \right)^2}{\rho_l - \rho_v} = M_*^{-4}$
Labantsov 1963 [25]	$h = 0.075 \left[1 + 10 \left(\frac{\rho_v}{\rho_l - \rho_v} \right)^{0.67} \right] \left[\frac{kl^2}{v \sigma (T_{sat} + 273.15)} \right]^{0.33} \left(\frac{q}{A} \right)^{0.67}$
Stephan and Abdelsala 1980 [26]	For water $\frac{h D_b}{kl} = (0.24E + 7) \left(\frac{q D_b}{AKl} \right)^{0.673} \left(\frac{H_{fg} D_b^2}{K_l^2} \right)^{-1.58} \left(\frac{T_{sat} D_b C_{pl}}{K_l^2} \right)^{1.26} \left(\frac{\rho_l - \rho_v}{\rho_l} \right)^{5.22}$ For ammonia and fluids for refrigeration cycles $\frac{h D_b}{kl} = 267 \left(\frac{q D_b}{A k_l T_{sat}} \right)^{0.745} \left(\frac{\rho_v}{\rho_l} \right)^{0.581} \left(\frac{\alpha_l}{Kl} \right)^{0.533}$ General form of equation $\frac{h D_b}{kl} = 0.23 \left(\frac{q D_b}{A k_l T_{sat}} \right)^{0.647} \left(\frac{\rho_v}{\rho_l} \right)^{0.297} * \left(\frac{H_{fg} D_b^2}{\sigma^2} \right)^{0.371} \left(\frac{\rho_l \sigma^2}{\sigma D_b} \right)^{0.35} \left(\frac{\rho_l - \rho_v}{\rho_l} \right)^{-1.73}$
Nishikawa 1982 [27]	$h = \frac{31.4 p_c^{0.2}}{mw^{0.1} T_c^{0.9}} (8R_a)^{0.2} \left(1 - \frac{p}{p_c} \right) \frac{(p/p_c)^{0.23} (q/A)^{0.8}}{[1 - 0.99(p/p_c)]^{0.9}}$
Cooper 1984 [28]	$h = 55 p_r^{0.12 - 0.443 R_a} (-\log p_r)^{-0.55} m w^{-0.5} (q/A)^{0.67}$
Gorenflo 1993 [29]	$\frac{h}{h_0} = \left(\frac{q}{q_0} \right)^{n(p_r)} F(p_r) \left(\frac{R_p}{R_{a0}} \right)^{0.133}$
Alavi Faze 2010 [30]	$h = \frac{3.253 \sigma^{0.125} H_{fg}^{0.125} (q/A)^{0.876}}{T_{sat} \alpha_l^{0.145}}$
Igor Seicho Kiyomura 2017 [31]	$h = 154 \left[\left(\frac{C_{pl} T_{sat}}{h_{lv}} \right)^{1.72} \left(\frac{C_{pl} H_l}{K_l} \right)^{-0.34} \left(\frac{D_b q}{\mu_l h_{lv}} \right)^{0.62} \left(\frac{S}{L_b} \right)^{a4 - 0.05} \right] \times \frac{k_l}{L_b}$ $L_b = \left(\frac{C_{pl} H_l}{K_l} \right)^{1/2}$

time for heating replaced liquid layer to nucleation of next bubble in the same bubble generator. The bubble departure frequency of surface le was studied since the early 1960s [32].

EXPERIMENTAL SECTION

Apparatus

The main part of the laboratory setup includes an empty copper cylindrical heater with a medium surface roughness of 0.21 μm , stable roughness during tests, external diameter of 25 mm and an internal diameter of 13 mm and with a length of 180 mm that has been used as a heat transfer surface within a rectangular cube tank with a dimension of 180 mm \times 130 mm \times 350 mm. It is made of Pyrex glass with a 10 mm thickness and high thermal resistance. This vessel is insulated by glass wool to avoid thermal dissipation. There is an electrical element located

in the middle of a copper cylinder with a maximum power generation of 1 kW. To change the input voltage and temperature record of the heater, there is an autotransformer 10 KVA (Model MST) with an input of 220 V, A/C, and output of 0-300 V at 1 kW. The voltage range is 100-220 V and increases 20 V stepwise. The change time for voltage rise is about 3-5 min which is created for system stability from temperature changes. In order to measure the voltage value and consumed amps, a multi-meter is utilized in the range of 1 mV-1000 V and 0.1 μA -20 A. As shown in Fig. 1, to accurately record the existing temperature changes on the heater surface, the three numbers of the thermocouple are placed in three holes with an angle of 120° to each other that are located at the closest possible distance to the external diameter of the cylinder about 1 mm. The diameter of each hole is 2 mm and the depth

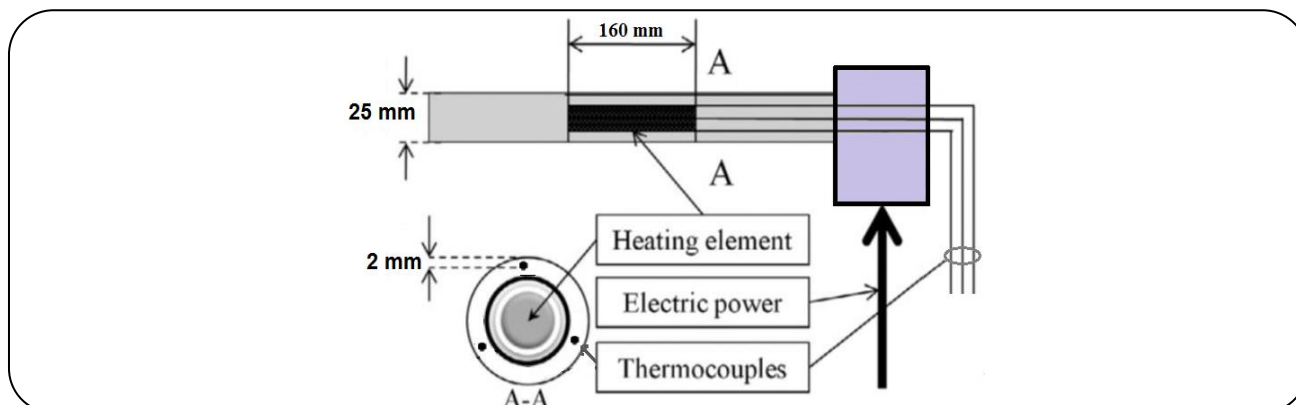


Fig. 1: Details of the heating heater.

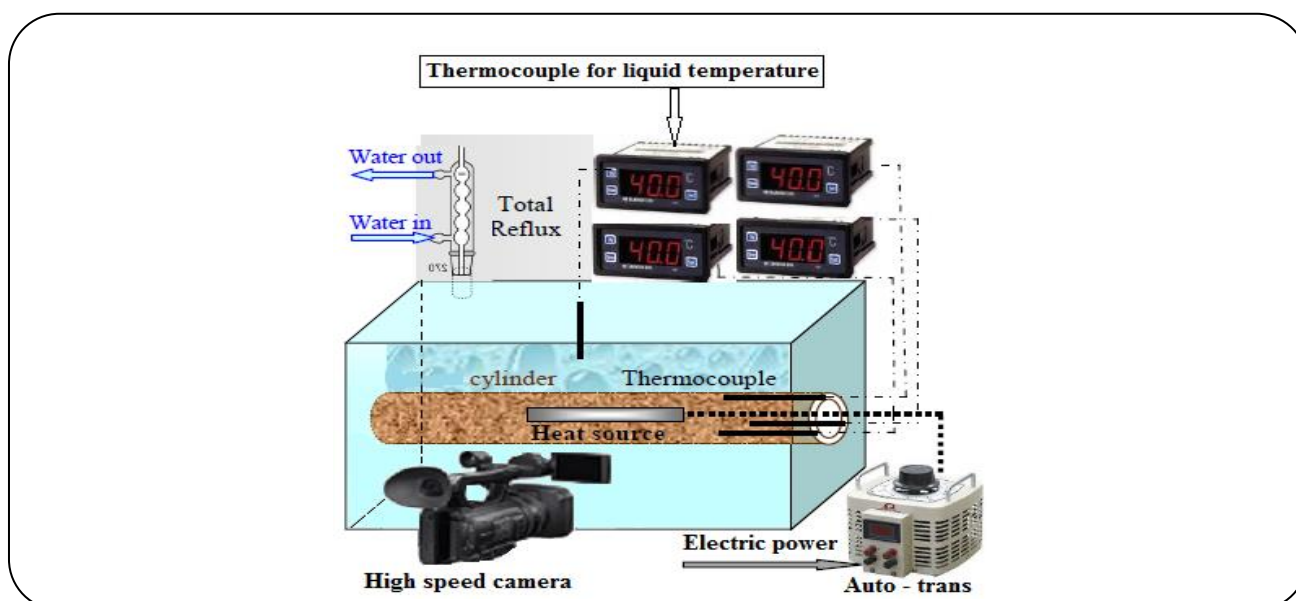


Fig. 2: The schematic of the experimental apparatus.

of them is 50 mm. Inside each hole, a K-type thermocouple with a length of 50mm, and a diameter of 2 mm, with a performance range from -180 to $+750$ °C and the sensitivity of about $41 \mu\text{V } ^\circ\text{C}^{-1}$ is placed. The temperature display is single-channel and LCD type, the model of HANYOUNG ED6-FKMAP4, with the ability to read the temperature in decimal accuracy. To prevent air penetration in the thermocouple holes, the silicon thermal with a conductivity of $4 \text{ W/m} \cdot ^\circ\text{C}$ was used so that there will be no significant viscosity reduction up to 230 °C.

Procedure

Initially, the setup system was cleaned and 2.5-liter deionized water was added and the solution reached the boiling point. In order to keep the boiling solution

volume, a condenser was placed on the top of the aquarium to condense produced vapors and return them to the aquarium. There is also a fourth thermocouple in bulk solution to make sure about the boiling of the solution during the tests. At each stage of experiments, the film is taken from the changes in the heat transfer surface and boiling solution by using a Sony PMW-300 K1 high-speed camcorder. An EDIUS software, film editing software, is used to observe and calculate the bubble dynamic changes including bubble departure frequency (by counting departure bubbles per time), bubble departure diameter (by averaging the diameter of a specific number of departure bubbles), and also active nucleation sites density (number of generators based on unit level). Physical properties of the heat transfer surface and deionized water are calculated by the heat

transfer surface temperature and solution. All experiments have been performed under atmospheric conditions, and to ensure repeatability, each heater surface slope was performed at least three times.

UNCERTAINTY AND DATA REDUCTION

The uncertainty of the heat transfer coefficient can be estimated by the Newton cooling law:

$$h = \frac{q/A}{(T_s - T_{sat})} \quad (2)$$

Heat flux was calculated by the following equation [33]:

$$q/A = V \cdot I \cdot \cos \varphi \quad (3)$$

Because of the linear shape of the heater section and the absence of any solenoid effect, the φ is assumed to be equal to unity. The maximum estimated uncertainty of heat flux would be equal to:

$$\frac{\delta(q/A)}{q/A} = \sqrt{\left(\frac{\delta I}{I}\right)^2 + \left(\frac{\delta V}{V}\right)^2} \quad (4)$$

Before estimating the uncertainty for heat transfer coefficient, δh , it is necessary to estimate the uncertainty of temperature difference, $\delta \Delta T$ by the following:

$$\delta \Delta T = \sqrt{(\delta T_s)^2 + (\delta T_{th})^2} \quad (5)$$

$$\frac{\delta h}{h} = \sqrt{\left(\frac{\delta I}{I}\right)^2 + \left(\frac{\delta V}{V}\right)^2 + \left(\frac{\delta T}{T}\right)^2} \quad (6)$$

The uncertainties of wall superheat temperature, can be derived by the integrated form Fourier's conduction equation in cylindrical coordination:

$$T_s = T_{th} - \frac{q \cdot b_s}{K_s} \quad (7)$$

In this equation, b_s is the distance between the thermocouple locations and the heat transfer surface and K_s is the thermal conductivity of the heater material

The results of the present uncertainty analysis for the experiment data are summarized in Table 2.

RESULTS AND DISCUSSION

In order to achieve a high heat transfer coefficient, the effects of changes in the heater slope, heat transfer surface,

Table 2: Uncertainty sources.

Parameter	Uncertainty
Tube diameter	± 0.01 mm
Tube length	± 0.01 mm
Thermocouple, K-type	± 0.1 °C
Voltage	± 1 V
Current	± 0.1 A
maximum heat flux of $76 \text{ kW}\cdot\text{m}^{-2}$	$\pm 1.8545 \text{ kW}\cdot\text{m}^{-2}$

the bubble dynamic in the process of bubble growth and changes are investigated. As was mentioned in the previous section, the bubble dynamics include the bubble departure frequency, bubble departure diameter, and active nucleation site density. Since there is no external force in pool boiling which could cause turbulence in the solution, the study of changes in these parameters in creating turbulence of the solution plays a significant role in rising heat transfer coefficient. According to experimental observations, when the slope of the heater surface rises, the bubble departure frequency and active nucleation site density, show a rising trend while the bubbles departure diameter is being declined. In the following, these incremental and declined changes are analyzed and their particular positive and negative effects on the heat transfer coefficient are studied.

Effect of the heater slope on the heat transfer coefficient

In this section, to investigate the effects of changes in the heater slope, zero slope is considered as a base model.

Increasing the slope of the heat transfer surface has a significant effect on increasing the heat transfer coefficient [34, 35]. As can be seen in Fig. 3 and Table 3, when heat transfer flux increases and the heater slope rises from 0° to 15° , the heat transfer coefficient goes up. Then, this incremental change in lower heat fluxes has a faster trend with respect to the high heat fluxes. Next following a 15° angle, the heat transfer coefficient begins to decline which indicates the 15° angle by a 20.1% increment and 30° angle by a 1.8% increment have the highest and lowest rate of changes in the heat transfer coefficient, respectively. The upward trend of the heat transfer coefficient in all angles rises up to $46 \text{ kW}/\text{m}^2$ with a faster rate, and followed by a slower trend, it reaches $76 \text{ kW}/\text{m}^2$. For instance, the heat flux has had an upward trend (with 24% average increment)

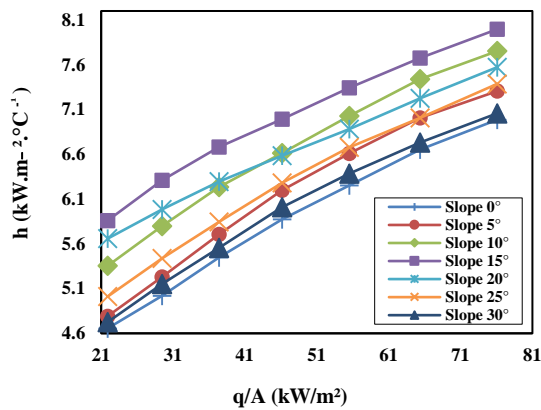


Fig. 3: Effects of the slope of the heater on the heat transfer coefficient at different heat fluxes.

up to $46 \text{ kW}\cdot\text{m}^{-2}$ in the 15° angle and following an average increase of 22%, it reaches up to $76 \text{ kW}\cdot\text{m}^{-2}$. Since the heat transfer coefficient is based on the departure frequency, departure diameter, and active nucleation sites density of bubbles, to understand the reason for increasing the heat transfer coefficient at the 15° angle, it is essential to study the effective parameters. That is, the performance conditions and the behavior of these three parameters along with the temperature changes, heat flux, and slope adjustments should be so that it can lead the system to increase higher heat transfer coefficient. On one hand, it should be noted that the higher the heat transfer coefficient, the faster the heater surface was cooled, and hence, the heat can be transferred to the solution more quickly. On the other hand, this declined temperature is not only caused by to transfer of the heat flux to a lower temperature, but also it prevents a rise in temperature and several probable damages such as corrosion, rust, and fouling of the heater surface. The reasons for the rise in heat transfer coefficient by the use of dynamic parameters of the bubble are explained as follows. *Pi et al.* in their experiments on the ramp from 0° to 90° indicated that the angle of 22° has the highest BHTC [36].

Effect of the heater slope on the active nucleation sites density

In this section, the first parameter, the active nucleation site density, and its effects on increasing the heat transfer coefficient are investigated.

In Fig. 4, it was obvious that there is a rise in the heater angle from 0° to 30° , and also, the increase of the heat flux

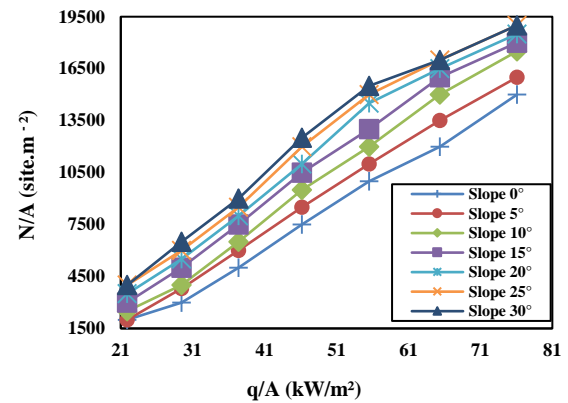


Fig. 4: Effects of the slope of the heater on the active nucleation site density at different heat fluxes.

has resulted in raising the active nucleation sites density. Following a 15° angle, the growth trend is considerably increased by 20% from the previous angle. As can be depicted in Table 3, it reaches 12 and 8 percent in the next angles. The upward trend of the active nucleation site density in the angles less than 15° can be assumed approximately linear. However, there is a more rapid trend in high heat fluxes when the slope in lower fluxes shows a remarkable increase from 20° to 30° . Whereas the growing trend of the production of active nucleation sites density in high fluxes was dropped and these three angles converged to one specific point. This drop may result in a saturated unit of the heater surface of the bubble. Likewise, the increasing trend of the active nucleation site density in all angles continues with a more rapid trend up to the heat flux of $76 \text{ kW}\cdot\text{m}^{-2}$. If the 15° would be re-analyzed, it was concluded that the heat flux of 46 and $76 \text{ kW}\cdot\text{m}^{-2}$ will be increased up to the average rise of 52 and 42 percent, respectively. Similar experimental results were also obtained by *Dadjoo et al* [18]. An important factor in reducing the heat transfer by slope increasing from horizontal to vertical is due to both merging bubbles and producing larger bubbles on the surface of the heater therefore, heat transfer resistance increases due to the formation of a layer of moving bubbles on the surface. Also, Jung and Kim Showed that the inclination of the boiling surface from horizontal to vertical increases nucleation site density [20].

As the bubble leaves the nucleate generator, it would be separated through slides and movements. When it slides for separating, in order to activate the springs, it could give

its steam microlayer to the adjacent active nucleation sites density of the bubble which is not active. Because one of the most significant factors of bubble generation is the presence of the steam microlayer in the active nucleation site density. According to research done by *Thgormcroft* [37], this slide of the bubble has a displacement up to 1.6 times the departure diameter which is resulted in activating more springs. This phenomenon in zero or very low angles occurs without any slight slide. On the one hand, an increase of the heat flux leads to activating a number of inactive springs which resulted in increasing the active nucleation sites density of the bubble and followed by more production of bubble volume in a unit area. It has been illustrated in previous studies that the rise of the active nucleation site density of the bubble has a considerable impact on the increase of turbulence [38]. At first, the rise of the heat transfer coefficient is caused to increase the number of the active nucleation sites density and secondly, the more bubble departure diameter, the more turbulence in the solution would be expected. But this increasing rate of the active nucleation sites density is not always suitable for the system. Although the compression of the active nucleation sites density is too excessive, the bubbles in the heat fluxes are connected to each other more rapidly on a heating surface and like an air cushion, it prevents the liquid to reach the heater surface which resulted in resisting the heat transfer [18, 19]. For this reason, it cannot be expected that a 30° angle would have a higher heat transfer coefficient despite the more active nucleation site density of the bubble.

Effect of the heater slope on the bubble departure frequency

The second important factor is the bubble departure frequency which is studied in this section. As can be indicated in Fig. 5, the bubble departure frequency like the active nucleation sites density has boomed remarkably by means of the heat flux and the heater angle. Regarding the rise of heat flux similar to the previous section, it should be stated that the rise of flux led to increasing energy and as a consequence, there is more power to produce more bubbles in time. By changing the angle, the buoyancy force helps the bubble and would cause it to separate the bubble from the surface more rapidly. However, this type of force has a few effects on lower angles than the higher ones.

As can be observed in Fig. 5, following a 20° angle, the bubble departure frequency begins to increase exponentially.

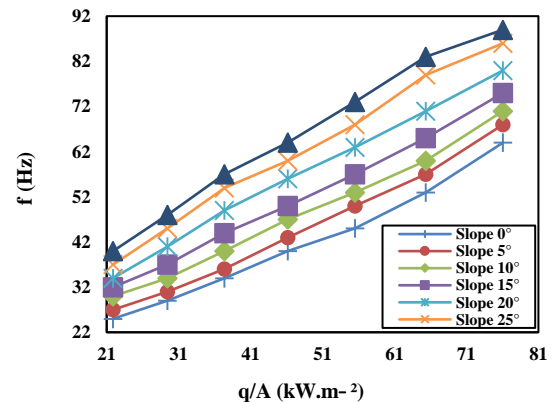


Fig. 5: Effects of the slope of the heater on the bubble departure frequency at different heat fluxes.

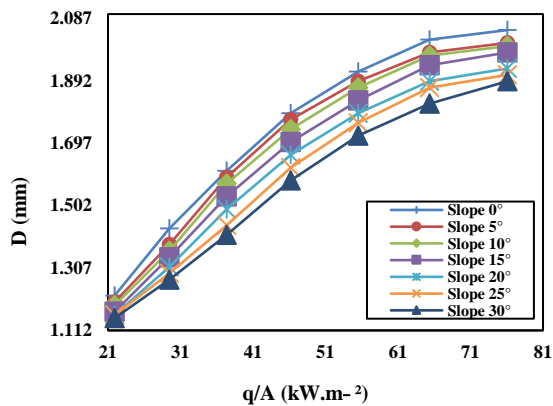
This incremental trend will be boosted up to the flux of 46 kW/m² similar to the active nucleation site density in all angles, and followed by a lower trend, it goes up to 76 kW/m². In the 15° angle, this departure frequency is increased up to 46 kW/m² (with an average rate of 28%) and then, it continues with a 22% average rate up to 76 kW/m². The higher the departure frequency, the more active nucleation site density would be expected which can cause to rise more turbulence in the solution. *Parul et al.* found that the departure frequency increased with an increase in inclination angle [22]. Therefore, it should be noted that bubble production is in favor of the increase of heat transfer coefficient, and the bubble departure diameter changes are investigated in the following section and its relationship with the bubble departure frequency will be analyzed.

Effect of the heater slope on the bubble departure diameter

The investigation of changes in the third effective parameter of the heat transfer coefficient, the bubble departure diameter, was carried out. As it is clear in Fig. 6 and Table 3, the diameter changes are being increased by the rise of heat flux, but it has a converse relationship with the angle. It simply means that the more the heater angle, the less the bubble departure diameter so that the largest bubbles are produced in the horizontal mode or zero degrees. This is due to the presence of buoyance force which was explained in the previous section that was caused to increase the bubble departure frequency. It basically means that the bubbles leave the surface faster and have a limited time to grow on the surface, therefore

Table 3: Effect of the slope changes on the heat transfer coefficient and bubble dynamics.

Slope	5°	10°	15°	20°	25°	30°
Fluctuation h%	4.7	13.3	20.1	13.7	6.9	1.8
Fluctuation N/A%	12.7	25.2	44.4	53.0	64.1	69.5
Fluctuation f%	7.6	16.4	25.2	37.2	49.5	58.7
Fluctuation D%	-0.3	-2.9	-4.6	-6.7	-8.2	-9.9

**Fig. 6: Effects of the slope of the heater on the departure diameter of the bubbles at different heat fluxes.**

the bubble remains small in size. In this parameter, unlike the active nucleation sites density, the upward trend of the bubble departure diameter was extremely declined in all angles up to 46 kW/m² and it has been followed by 76 kW/m² in the flux. It was reduced with a 5% average rate in a 15° angle up to 46 kW/m² and followed by 76 kW/m² with an average decrease of 5.6%. This decrease in the bubble diameter with increasing angle is similar to obtained results by Xiaoyue Pi [36].

One significant factor in the bubble performance to increase the heat transfer coefficient is that the production of the bubble departure diameter has two important effects. Firstly, when the bubble is separated from the surface and moves up, the larger diameter bubbles can cause more turbulence. Secondly, the produced steam inside of each bubble when growing, its temperature would be equal to the temperature of the heater surface. So the larger bubble, the more heat is separated from the surface, and it cools the surface more rapidly than a bubble with a smaller diameter. Hence, these two parameters imply the importance and effectiveness of the bubble with a larger diameter. The produced bubble diameter has a converse relationship with the bubble departure frequency which

means the more bubble departure frequency, the smaller bubbles would be imagined.

Ivey [39] presented a basic relationship between the produced bubble departure diameter and the bubble departure frequency as follows:

$$f_b \propto D_b^{-n} \quad (8)$$

In which n is equal to 0.5, 1, or 2, considering the above equation, the bubble departure frequency (f_b) is increased as the bubble departure diameter (D_b) declined.

These factors could prove that a more bubble departure frequency doesn't necessarily bring increasing the heat transfer coefficient. In order to study these three parameters about the 15° angle as the best performance Fig. 7, the following results should be noted:

First and foremost, it is worth mentioning that a rise in the active nucleation sites density is the benefit for the system, but this incremental rate is suitable to the extent that these sites wouldn't be so close together. The connection of these sites acts like a resistance that may prevent the solution to reach the heater surface and result in raising the temperature of the heater surface. Meanwhile, there is an approximate increase of 45% in producing the active nucleation sites density in the 15° angle with regard to 0° surface which proved that this increase is the best performance. The second important factor is related to the bubble departure frequency. Although an increase in the bubble departure frequency can cause to rise in the turbulence of the solution, raising the departure frequency decreases the bubble departure diameter on the heater surface. The 15° angle with an approximate increase of 25% in the departure frequency has only led to reducing the bubble departure diameter up to 4.4%. In addition, every time when there is a rise in angle in the heat transfer coefficient, it causes more losing accessibility of boiling solution to the heat transfer coefficient. Fig. 8 indicates three angles of 0°, 15°, and 30°.

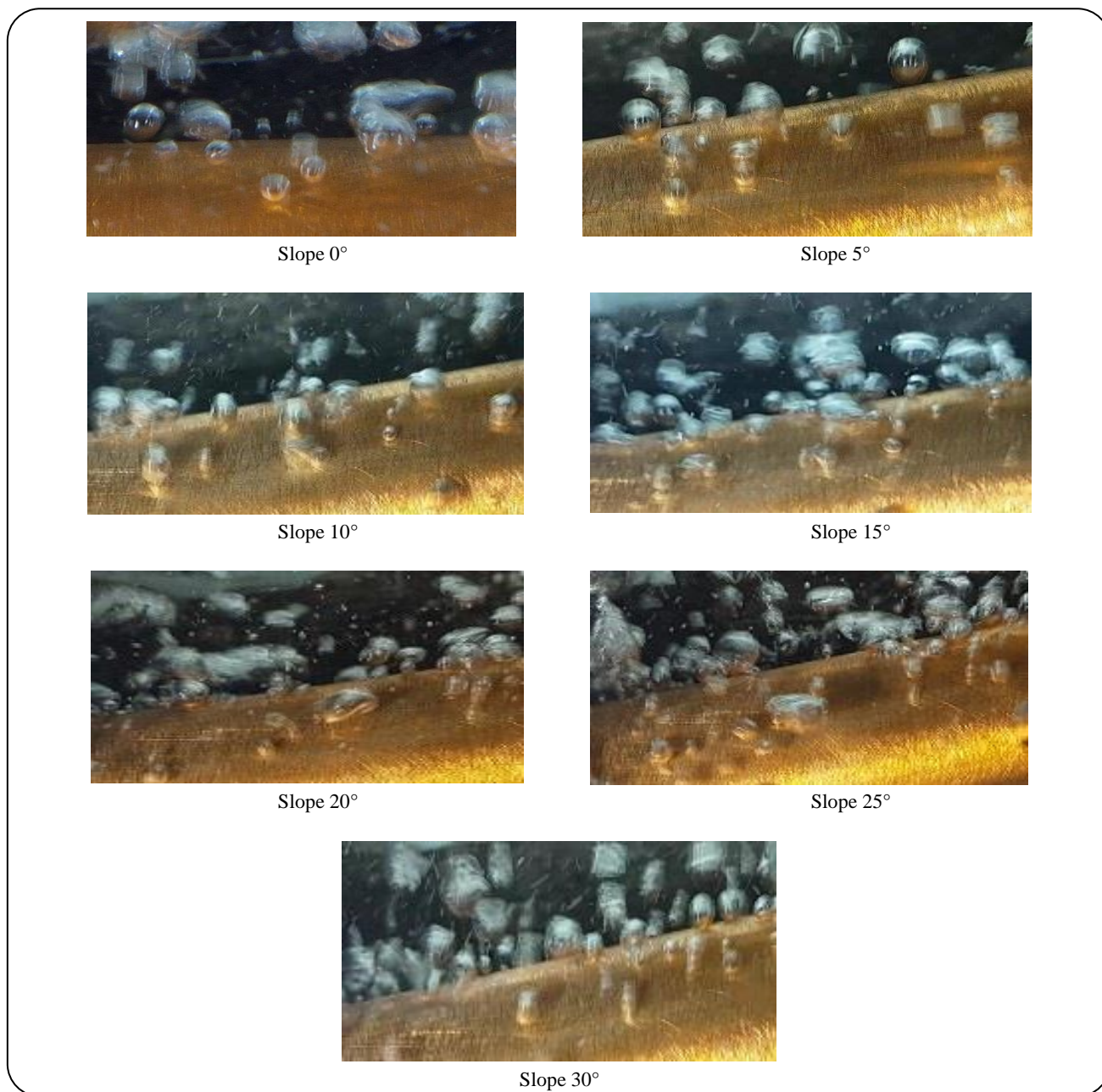


Fig. 7: Changes of bubble growth on the tested surfaces in the heat flux 37 (kW/m²).

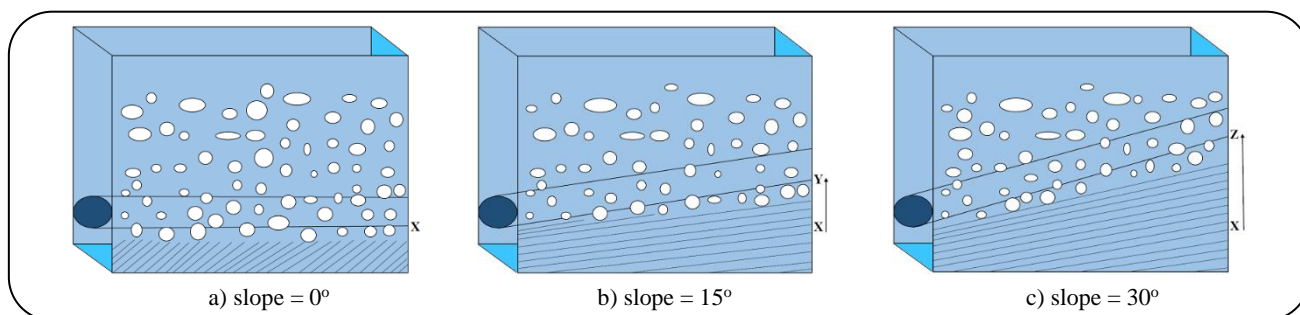


Fig. 8: Schematic of the variation of the heater slope.

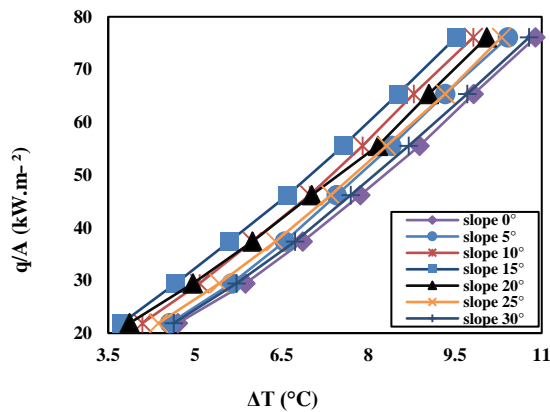


Fig. 9: Effect of the heater slope of the superheated wall on the heat flux at different temperature differences.

It is noticeable in Fig. 8, that as the cylinder slope (the heat transfer surface) rises, a great amount of the solution under the cylinder surface (the hatched zone) remains motionless. Despite the fact that the increase of the slope part of the solution can take out from the boiling zone, its amount up to a 15° angle can't be so considerable with regard to the influence of parameters such as the departure frequency, diameter, and the active nucleation sites density. Following a 15° angle, it has a direct effect on heat transfer. The change of these four parameters (the slope, diameter, departure frequency, and the active nucleation sites density) together cause the 15° angle to be an optimized slope. Moreover, in the optimum slope, the heater surface can transfer the same amount of heat in lower temperatures as compared to the other slopes. The more constant and specific the heat flux value, the less heat loss is inflicted on the heat transfer surface [32]. In order to have a better understanding of the effect of slope on the rise of the heat transfer coefficient, the reduction of temperature difference ($\Delta T_{\text{sat}} = T - T_s$) to exchange the same amount of the heat flux, and the effects of the evaluated surfaces are investigated in Fig. 9.

As it is recognizable that the 15° angle, which was introduced as an optimized slope in the previous sections, has less temperature difference than other slopes at the same heat flux. It has been able to transfer the same amount of the produced heat flux to the heat transfer surface and this decreased temperature has resulted in raising the heat transfer coefficient at the 15° angle. The heat transfer coefficient obtained through the experiments at the 15° angle is studied in the following section. Fig. 10 illustrates this comparative analysis.

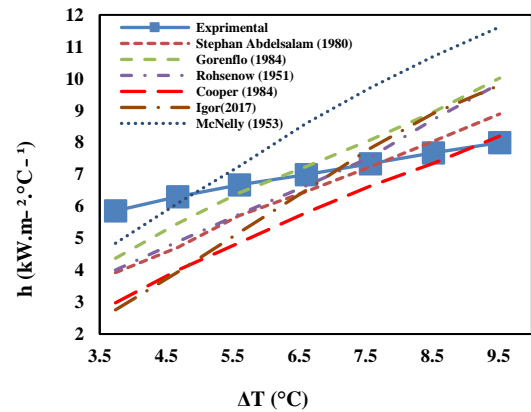


Fig. 10: Experimental and predicted pool boiling heat transfer coefficient for the pure water in the 15° slope of the heater.

According to Fig. 10 and the results of the error percent in Table 4, it is observed that the Stephan Abdelsalam model has an adequate overlapped with the experimental results and the minimum error is equal to 13.9%.

CONCLUSIONS

In this study, the effects of the heater slope on the heat transfer coefficient were verified at 0°, 5°, 10°, 15°, 20°, 25°, and 30° with an average roughness of 0.21 μm in a deionized water solution. The results have intensified that by increasing the slope up to 15°, the heat transfer coefficient had an incremental process, and afterward, up to 30° has taken a downward trend. It was found that the best results were obtained on the slope of 15° with an average increase of 20% compared to 0° slope. It was illustrated in surveys that increasing dynamic factors of bubble production, which contains diameter, frequency, and active nucleation sites density, by causing turbulence in solution has a crucial impact on increasing heat transfer. Although increasing all these parameters is not always beneficial for the heat transfer rate. As if the active nucleation site density increase consumedly the surface of the heater will be covered as a result and prevents liquid from reaching the surface of the heater. Besides increasing the bubble departure frequency causes a decrease in bubble departure diameter, and a further decrease in bubble departure diameters has a direct impact on the heat transfer coefficient reduction. Since bigger-sized bubbles have a more vital role in solution turbulence and heat separation from the heater surface, compared to bubble departure frequency growth. These three parameters have been optimized in 15° slope. In the following comparison between

Table 4: The model error of the experimental data for pure water in the 15° slope of the heater.

Slope	Stephan Abdelsalam (1980)	Gorenflo (1984)	Rohsenow (1951)	Cooper (1984)	Igor (2017)	McNelly (1953)
Error %	13.9	14.0	16.1	20.5	23.6	24.2

previous relationships of the heat transfer presentation and experimental results had taken that Abdelsalam's model had the minimum error and the best overlapping with the experimental data.

Nomenclature

A	Area, m ²
B	Distance, m
C_p	Heat capacity, J/(kg.°C)
C_r	Fixed coefficient of Rohsenow equation
D	Bubble departing diameter, mm
F	Bubble departing frequency Hz
F_p	Parameter of Mostinski equation
	Heat transfer coefficient, W/(m ² .°C)
H_{fg}	Specific heat of vaporization, J/kg
I	Current, A
I^*	Parameter of Kutateladze equation
K	Thermal conductivity, W/(m.°C)
M^*	Parameter of Kutateladze equation
M_w	Molecular weight, kg/koml
P	Pressure, Pa
P_c	Critical pressure
P_R	Reduced pressure
Q	Heat, W
R_a	Roughness average, μm
S	Surface
T	Temperature, °C
T_c	Critical temperature
t	Time, S
g_c	Correction coefficient of incompatible units, $\frac{Lb_m ft}{Lb_f s^2}$
V	Voltage, v

Greek symbols

$\hat{\alpha}$	Thermal diffusivity, m ² /s
β'	Fixed coefficient of Rohsenow equation
δ	Heat penetration depth, m
ρ	Density, kg/m ³
μ	Viscosity, kg/ms
σ	Surface tension, N/m
π	Pi number
φ	Phase difference between voltage and electrical current

Δ

Difference

Subscripts or superscripts

0	Base
B	Bubble
c	Critical
g	Growing
l	Liquid
sat	Saturation
th	Thermometers
v	Vapor
w	Wall

Received : Mar. 25, 2020 ; Accepted : Jun. 4, 2020

REFERENCES

- [1] Alavi Fazel S.A., Jamialahmadi M., Safekordi, A.A., [Experimental Investigation in Pool Boiling Heat Transfer of Pure/Binary Mixtures and Heat Transfer Correlations](#), *Iran. J. Chem. Chem. Eng. (IJCCE)*, **27(3)**: 135-150 (2008).
- [2] Zhou J., Zhang Y., Wei J., [A Modified Bubble Dynamics Model for Predicting Bubble Departure Diameter on Micro-Pin-Finned Surfaces under Microgravity](#), *Appl. Therm. Eng.*, **132**: 450-462 (2018).
- [3] Jafari Nasr M.R., Rahaei N., [Improving Heat Transfer in Falling Film Evaporators in Food Industries](#), *Iran. J. Chem. Chem. Eng. (IJCCE)*, **38(4)**: 237-250 (2019).
- [4] Sur A., Lu Y., Pascente C., Ruchhoeft P., Liu D., [Pool boiling Heat Transfer Enhancement with Electrowetting](#), *Int. J. Heat Mass Transfer*, **120**: 202-217 (2018).
- [5] Rahaei N., Jafari Nasr M.R., [Improving Heat Transfer in Falling Film Evaporators in Food Industries](#), *Iran. J. Chem. Chem. Eng. (IJCCE)*, **36(4)**: 237-250 (2019).
- [6] Alavi Fazel S.A., Jamialahmadi M., Safekordi A.A., [Experimental Investigation in Pool Boiling Heat Transfer of Pure/Binary Mixtures and Heat Transfer Correlations](#), *Iran. J. Chem. Chem. Eng. (IJCCE)*, **27(3)**: 135-150 (2008).

- [7] Emery T.S., Jaikumar A., Raghupathi P., Joshi I., Kandlikar S.G., [Dual Enhancement in HTC and CHF for external Tubular Pool Boiling - A Mechanistic Perspective and Future Directions](#), *Int. J. Heat Mass Transfer*, **122**: 1053-1073 (2018).
- [8] Chun M-H., Kang M-G., [Effects of Heat Exchanger Tube Parameters on Nucleate Pool Boiling Heat Transfer](#), *J. heat transfer*, **120(2)**: 468-476 (1998).
- [9] Kang M-G., [Effect of Surface Roughness on Pool Boiling Heat Transfer](#), *Int. J. Heat Mass Transfer*, **43(22)**: 4073-4085 (2000).
- [10] Kang M-G., [Effects of Tube Inclination on Pool Boiling Heat Transfer](#), *Nucl. Eng. Des.*, **220(1)**: 67-81 (2003).
- [11] Kang M-G., [Effects of the Inclination Angle on Pool Boiling in an Annulus](#), *Int. J. Heat Mass Transfer*, **51(19-20)**: 5018-5023 (2008).
- [12] Kang M-G., [Pool Boiling Heat Transfer on the Tube Surface in an Inclined Annulus](#), *Int. J. Heat Mass Transfer*, **53(15-16)**: 3326-3334 (2010).
- [13] Kang M-G., [Variation of Local Pool Boiling Heat Transfer Coefficient on 3-Degree Inclined Tube Surface](#), *Nucl. Eng. Technol.*, **45(7)**: 911-920 (2013).
- [14] Prakash Narayan G., Anoop K.B., Sateesh G., Das SK., [Effect of Surface Orientation on Pool Boiling Heat Transfer of Nanoparticle Suspensions](#), *Int. J. Multiphase Flow*, **34(2)**: 145-160 (2008).
- [15] Sateesh G., Das S.K., Balakrishnan A.R., [Experimental Studies on the Effect of Tube Inclination on Nucleate Pool Boiling](#), *Heat Mass Transfer*, **45(12)**: 1493-1502 (2009).
- [16] Parker J.L., El-Genk M.S., [Saturation Boiling of HFE-7100 Dielectric Liquid on Copper Surfaces with Corner Pins at Different Inclinations](#), *J. Enhanc. Heat Transf.*, **16(2)**: 103-122 (2009).
- [17] Zhong D., Sun J., Meng Ja., Li. Z., [Effects of Orientation and Structure Geometry on Boiling Heat Transfer for Downward Facing IGTAC Surfaces](#), *Int. J. Heat Mass Transfer*, **123**: 468-472 (2018).
- [18] Dadjoo M., Etesami N., Esfahany MN. [Influence of Orientation and Roughness of Heater Surface on Critical Heat Flux and Pool Boiling Heat Transfer Coefficient of Nanofluid](#), *Appl. Therm. Eng.*, **124**: 353-361 (2017)
- [19] Priarone, A., [Effect of Surface Orientation on Nucleate Boiling and Critical Heat Flux of Dielectric Fluids](#), *Int. J. Therm. Sci.*, **44(9)**: 822-831 (2005).
- [20] Jung S., Kim H., [Effects of Surface Orientation on Nucleate Boiling Heat Transfer in a Pool of Water Under Atmospheric Pressure](#), *Nucl. Eng. Des.*, **305**: 347-358 (2016).
- [21] Goel P., Nayak A.K., Kulkarni P.P., Joshi J.B., [Experimental Study on Bubble Departure Characteristics in Subcooled Nucleate Pool Boiling](#), *Int. J. Multiphase Flow*, **89**: 163-176 (2017).
- [22] Rohsenow W.M., [A Method of Correlating Heat Transfer Data for Surface Boiling of Liquids](#), Cambridge, Mass.: MIT Division of Industrial Cooperation, (1951).
- [23] McNelly M., [A Correlation of Rates of Heat Transfer to Nucleate Boiling of Liquids](#), *J. Imperial College Chem. Eng. Soc.*, **7**: 18 (1953).
- [24] Kutateladze S.S., [Heat Transfer in Condensation and Boiling](#), *AEC-tr-3770*. (1959).
- [25] Labunstov D., [Mechanism of Vapor Bubble Growth in Boiling on the Heating Surface](#), *J. Eng. Phys. Thermophys.*, **6(4)**: 33-47 (1963).
- [26] Stephan K., Abdelsalam M., [Heat-Transfer Correlations for Natural Convection Boiling](#), *Int. J. Heat Mass Transfer*, **23(1)**: 73-87 (1980).
- [27] Nishikawa K., Fujita Y., Ohta H., Hitaka S., [Effects of System Pressure and Surface Roughness on Nucleate Boiling Heat Transfer](#), *Kyushu University*, **42(2)**: 95-123 (1982).
- [28] Cooper M., [Saturation Nucleate Pool Boiling a Simple Correlation](#), *Paper Presented at IChemE Symp., Ser'*, 785-793 (1984).
- [29] Gorenflo D., [Pool Boiling, VDI Heat Atlas](#), VDI-Verlag, Dusseldorf, Germany (1993).
- [30] Alavi Fazel S.A., Roumana S., [Pool Boiling Heat Transfer to Pure Liquids](#), *Continuum Mechanics, Fluids, Heat*, 211-216 (2010).
- [31] Kiyomura I.S., Mogaji T.S., Manetti L.L., Cardoso E.M., [A Predictive Model for Confined and Unconfined Nucleate Boiling Heat Transfer Coefficient](#), *Appl. Therm. Eng.*, **127**: 1274-1284 (2017).
- [32] Zuber N., [Hydrodynamic Aspects of Boiling Heat Transfer](#), Los Angeles, CA, United States, Univ. of California (1959).
- [33] Alavi Fazel S.A., [A Genetic Algorithm-Based Optimization Model for Pool Boiling Heat Transfer on Horizontal Rod Heaters at Isolated Bubble Regime](#), *Heat Mass Transfer*, **53(9)**: 2731-2744 (2017).

- [34] Khooshehchin M., Mohammadidous A., Ghotbinasab S., [An Optimization Study on Heat Transfer of Pool Boiling Exposed Ultrasonic Waves and Particles Addition](#), *Int. Commun. Heat Mass Transfer*, **114**: 104558 (2020).
- [35] Mei Y., Shao Y., Gong S., Zhu Y., Gu H., [Effects of Surface Orientation and Heater Material on Heat Transfer Coefficient and Critical Heat Flux of Nucleate Boiling](#), *Int. J. Heat Mass Transfer*, **121**: 632-640 (2018).
- [36] Pi X., Rangwala A.S., [The Influence of Wire Orientation During Nucleate Pool Boiling in Subcooled Dodecane](#), *Int. J. Heat Mass Transfer*, **137**: 1247-1257 (2019).
- [37] Thorncroft G.E., Klausner J.F., Mei R., [An Experimental Investigation of Bubble Growth and Detachment in Vertical Upflow and Downflow Boiling](#), *Int. J. Heat Mass Transfer*, **41(23)**: 3857-3871 (1998).
- [38] Khooshehchin M., Salimi F., Jahangiri A., [The Influence of Surface Roughness and Solution Concentration on Pool Boiling Process in Diethanolamine Aqueous Solution](#), *Heat Mass Transfer*, **54(10)**: 2963–2973 (2018).
- [39] Ivey H.J., [Relationships between Bubble Frequency, Departure Diameter and Rise Velocity in Nucleate Boiling](#), *Int. J. Heat Mass Transfer*, **10(8)**: 1023-1040 (1967).